

Supporting Materials to:

**Magnetic quantification of single-crystalline Fe and Co nanowires via
off-axis electron holography**

Ke Chai^{1,2}, Zi-An Li^{2,a}, Wenting Huang³, Gunther Richter³, Ruibin Liu^{1,b}, Bingsuo Zou^{1,c}, Jan Caron⁴, András Kovács⁴, Rafal E. Dunin-Borkowski⁴ and Jianqi Li²

¹ Beijing Key Laboratory of Nano photonics and Ultrafine Optoelectronic Systems, School of Physics, Beijing Institute of Technology, Beijing 100081, P. R. China

² Beijing National Laboratory for Condensed Matter Physics and Institute of Physics, Chinese Academy of Sciences, Beijing 100190, P. R. China

³ Max Planck Institute for Intelligent Systems, Heisenbergstrasse 3, D-70569 Stuttgart, Germany.

⁴ Ernst Ruska-Centre for Microscopy and Spectroscopy with Electrons and Peter Grünberg Institute, Forschungszentrum Jülich, D-52425 Jülich, Germany.

*Corresponding authors

E-mail: zali79@iphy.ac.cn (Zi-An Li),

liuruibin8@gmail.com (Ruibin Liu),

zoubs@bit.edu.cn (Bingsuo Zou).

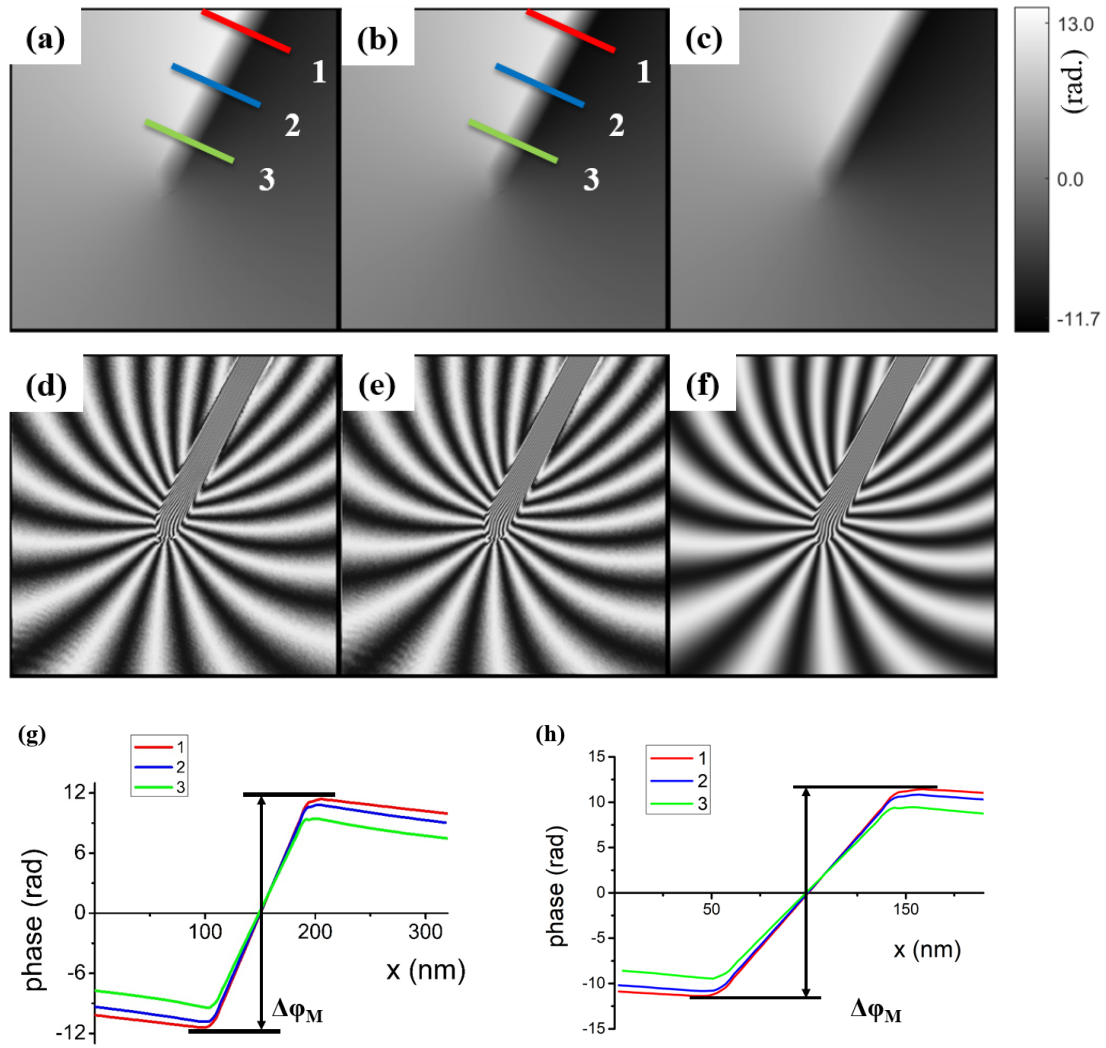


Fig. S1. (a-c) are the respective magnetic phase images of the apex part of Fe NW of the original, the corrected one after removing linear phase ramp, and the reconstructed one generated from the reconstructed magnetization. The lines (red, blue and green) mark the positions for the phase profile extraction. (d-f) are the equal-phase maps constructed by 5x-amplified magnetic phase images of the respective (a-c), displaying the projected in-plane magnetic induction field distributions inside and around the Fe NW. (g-h) are the line profiles of phase images marked in (a-b).

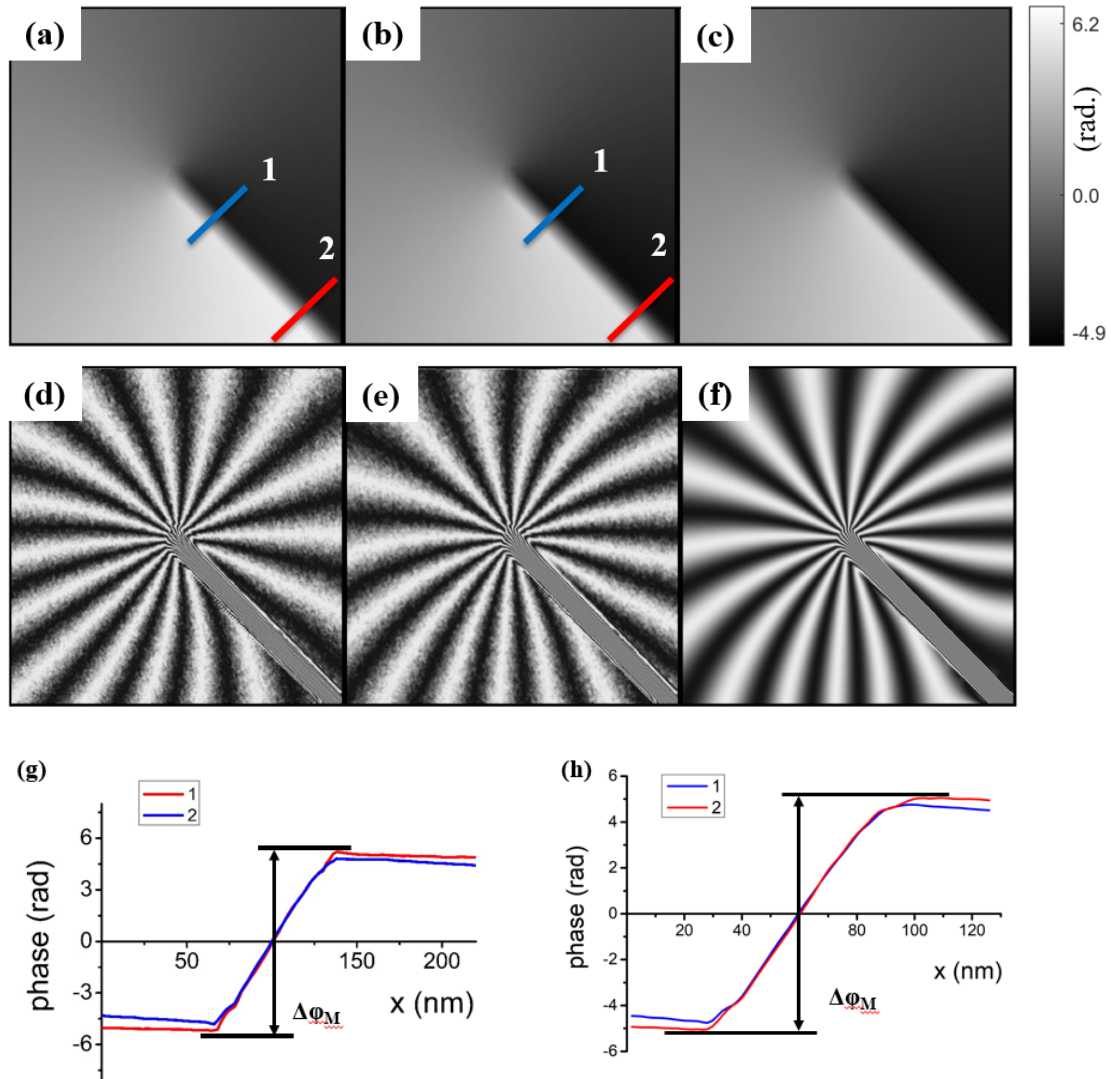


Fig. S2. (a-c) are the respective magnetic phase images of the apex part of Co NW of the original, the corrected one after removing linear phase ramp, and the reconstructed one generated from the reconstructed magnetization. The lines (red and blue) mark the positions for the phase profile extraction. (d-f) are the equal-phase maps constructed by 10x-amplified magnetic phase images of the respective (a-c), displaying the projected in-plane magnetic induction field distributions inside and around the Co NW. (g-h) are the line profiles of phase images marked in (a-b).

Figure S1(a-c) and S2(a-c) display the phase images of the original (as-reconstructed from hologram), the corrected one after removal of linear phase ramps, and the recalculated one from the reconstructed magnetization distributions for the Fe and Co NWs, respectively. To estimate the difference in the magnetization measurements using the different phase images (the original and the corrected ones) shown in Fig. S1(a-c) and S2(a-c), we plot the phase profiles in these phase images and measure the corresponding magnetic induction using the following expression,

$$B = \frac{\hbar\Delta\Phi_M}{eS}$$

Our measurements for both Fe and Co NWs show that there is a very slight difference in magnetization determinations between the original and the corrected ones: 0.13% for Fe and 0.35% for Co. These small differences are likely associated with the small amount of the phase ramps presented in the original magnetic phase images and the fact that only a small portion of phase across the wire is used for estimation of magnetization.

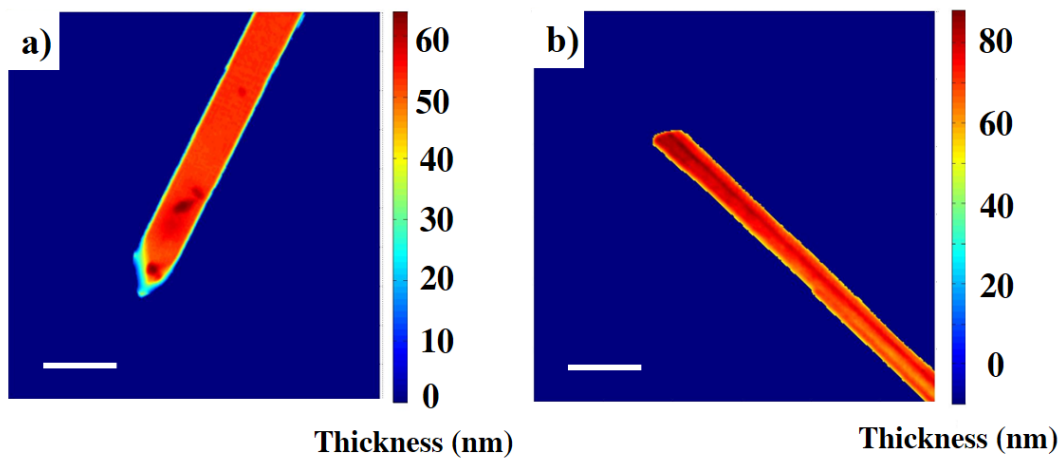


Fig. S3. The extent of thickness variations of (a) the Fe NW and (b) the Co NW based on the phase shift of electrostatic potential. The scale bars correspond to 200nm.

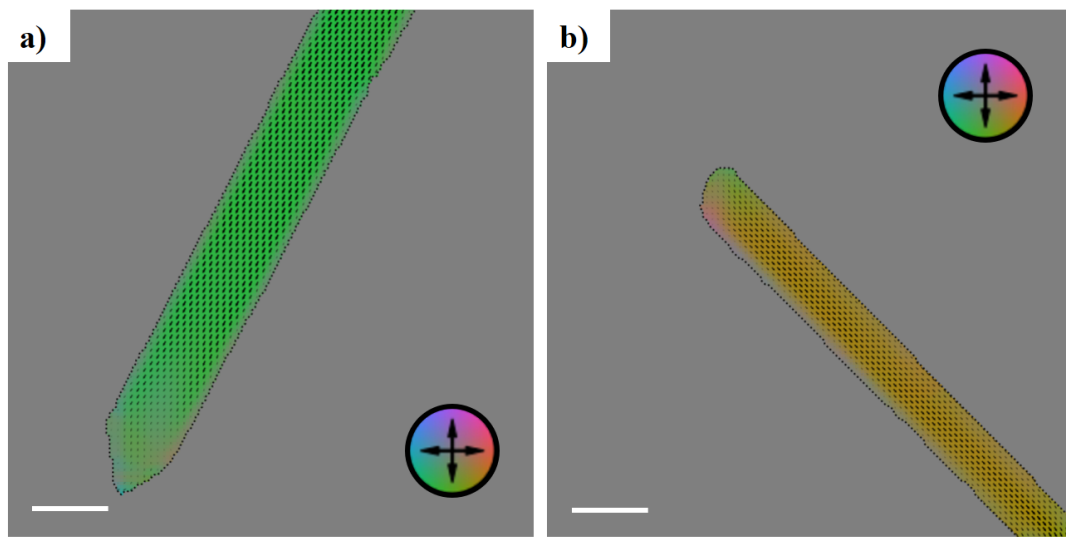


Fig. S4. Projected magnetization distributions of the apex part of (a) the Fe NW and (b) the Co NW. The color code is used to indicate the direction of the magnetization, and the scale bars correspond to 100nm.

Due to the magnetic stray field, removing a possible phase ramp from the magnetic phase images is not a trivial task, as no field-free vacuum region exists for conventional ramp fitting algorithms. Instead, a model-based iterative reconstruction algorithm¹⁻³ is used to fit a magnetic phase ramp and offset together with the magnetization distribution inside the Fe and Co NWs. This algorithm utilizes known analytic solutions for the phase of simple magnetic geometries and a priori information about the NWs position gained from the mean inner potential. Magnetic moments outside the Field of View (FOV) are taken into account by allowing the algorithm to fit magnetization to buffer zones directly outside the FOV, which can be safely discarded after reconstruction.

REFERENCE

- ¹ J. Caron, Ph. D dissertation (RWTH Aachen University, Germany, 2017).
- ² J. Caron, J. Ungermann, A. Kovács, P. Diehle and R.E Dunin-Borkowski, *Microscopy and Microanalysis* **25**,1806 (2019).
- ³ R.E Dunin-Borkowski, J. Caron, P. Diehle, A. Tavabi and A. Kovács, *Microscopy and Microanalysis*, **24**,108 (2018).